

# Conservation of energy in coherent backscattering of light

S. Fiebig<sup>(1)</sup>, C.M. Aegerter<sup>(1)</sup>, W. Bührer<sup>(1)</sup>, M. Störzer<sup>(1)</sup>, E. Akkermans<sup>(2)</sup>, G. Montambaux<sup>(3)</sup>, and G. Maret<sup>(1)</sup>

<sup>(1)</sup> *Fachbereich Physik, University of Konstanz, Box M621, 78457 Konstanz, Germany*

<sup>(2)</sup> *Department of Physics, Technion Israel Institute of Technology, 32000 Haifa, Israel*

<sup>(3)</sup> *Laboratoire de Physique des Solides, CNRS UMR 8502, Université Paris-Sud, 91405 Orsay, France*

(Dated: March 21, 2022)

Although conservation of energy is fundamental in physics, its principles seem to be violated in the field of wave propagation in turbid media by the energy enhancement of the coherent backscattering cone. In this letter we present experimental data which show that the energy enhancement of the cone is balanced by an energy cutback at all scattering angles. Moreover, we give a complete theoretical description, which is in good agreement with these data. The additional terms needed to enforce energy conservation in this description result from an interference effect between incident and multiply scattered waves, which is reminiscent of the optical theorem in single scattering.

Conservation of energy is one of the most fundamental principles in physics. Not only in mechanics, but also in thermodynamics it rests on fundamental symmetries, which so far have not been violated. There have however been instances, where novel effects gave rise to suspicions of non-conservation of energy as in the distribution of positron energies in beta decay. This was only explained by the introduction of the neutrino in Fermi's four-point theory [1]. Another instance which seemingly contradicts the conservation of energy is the coherent backscattering cone which appears when waves propagate in turbid media. In that case, a twofold enhancement of the backscattered intensity with respect to Lambert's law for diffusive scattering is observed. This enhancement decays over an angular scale of  $(kl^*)^{-1}$ , where  $k$  is the wavenumber of the wave and  $l^*$  is the transport mean free path of the medium [2]. Due to its fundamental nature, it can be observed in areas as different as solid state physics [3], soft matter physics [4], astro- [5] and geophysics [6], and with various kinds of waves like sound waves [7], microwaves [8] and, as in the experiments presented in this letter, visible light [4, 9].

The additional energy contribution of the coherent backscattering cone to the intensity can however not be explained by a corresponding reduction in transmission at surfaces not considered in the experiment. Rather, the backscattering cone is also observed from samples which can theoretically as well as experimentally be treated as filling an infinite half-space, meaning that the waves can reach no other surface than the one considered [2]. Moreover, different polarization channels also show a backscattering cone [10], such that the energy in the cone cannot be obtained from another polarization channel.

The origin of the backscattering cone lies in the interference of waves propagating along reciprocal paths. This interference can only spatially re-distribute the backscattered energy. Thus the energy enhancement at small angles has to be accompanied by a corresponding energy cutback to ensure conservation of energy. However, such an energy cutback has so far not been observed experimentally. Moreover, it is not described by the prevailing theories [2, 10, 11]. This can be problematic as the scal-

ing of the width of the backscattering cone with  $kl^*$  is commonly used to characterize multiple scattering materials. In particular in turbid samples, when the cone becomes very broad, there has to be a sizeable correction if conservation of energy is to hold. This is of great importance in the study of Anderson localization of light [12], where a reliable knowledge of the parameter  $kl^*$  is needed to characterize the phase transition from diffusive transport to an insulating state [13, 14].

In this letter, we present measurements of coherent backscattering, where the incoherent background is determined on an absolute scale. With this we are able to show that there is a reduction in backscattering intensity at all angles compensating for the enhancement in the back-direction. A theoretical description which fits these data shows that the reduction in enhancement results from a new interference effect between the incident and multiply scattered waves. This is analogous to the shadow term, which accounts for flux conservation in the optical theorem [15]. In multiple scattering, the terms needed to ensure energy conservation correspond to the so-called Hikami box or quantum crossing [16, 17]. The present experiment constitutes a direct observation of a scattering process described by a Hikami box, which plays a central role in quantum mesoscopic physics [17].

Our main setup to study the angular distribution of the backscattered light consists of 256 photosensitive diodes attached to a semi-circular arc with a diameter of 1.2m, in the center of which the sample is located [18]. In this way, we can detect light over a range of  $-60^\circ < \theta < 85^\circ$  with a resolution of  $0.14^\circ$  for  $|\theta| < 10^\circ$ ,  $\sim 1^\circ$  for  $10^\circ < |\theta| < 60^\circ$  and  $\sim 3^\circ$  for  $\theta > 60^\circ$ . For the illumination a continuous wave dye laser with a wavelength of 590 nm is used. The measurements are done using circularly polarized light in order to reduce the influence of single scattering. To average over random speckle patterns, the samples are rotated. As the very tip of the cone at  $\theta \simeq 0$  can not be resolved with this setup, the central part of the backscattering cone,  $|\theta| < 3^\circ$ , is measured separately using a beam splitter and a charge-coupled device (CCD) camera to a resolution of  $0.01^\circ$  [18].

In order to calibrate the photodiodes, we have used a

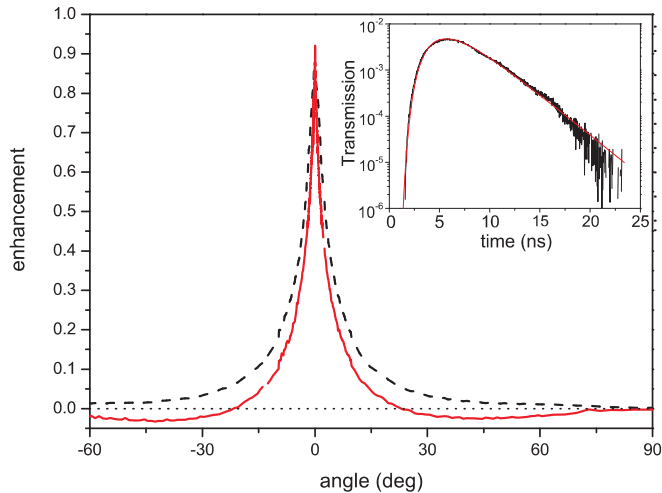


FIG. 1: Backscattering cone of R700 evaluated ignoring (dashed curve) and taking into account (full red curve) absorption in the reference sample. The former is positive for all angles, resulting in an uncompensated energy enhancement of the cone. For the latter, energy enhancement and energy cutback are balanced. This is quantified by the half-space integral of the intensity  $I = -0.005(7)$ . The inset shows a time of flight measurement of the teflon reference, which follows diffusion theory with an absorption time of 3.3 ns.

block of teflon as a reference sample. Teflon has a transport mean free path of  $\simeq 300 \mu\text{m}$  and hence the backscattering cone of teflon at a wavelength of 590 nm has a FWHM of about  $0.02^\circ$ , which is much narrower than the angular resolution of the wide-angle setup. This implies that with the wide-angle setup teflon can be considered as a purely incoherent signal, which is properly normalized given by  $\mu(\gamma + \mu/(\mu + 1))$  [17], where  $\mu = \cos \theta$  and  $\gamma l^*$  describes the distance over which the diffuse intensity enters the sample. These diode signals are measured at several different incident laser powers, which are determined independently with a calibrated power-meter. Interpolation of the measured data then yields a calibration function for each photodiode [18]. To be able to determine the intensity of the backscattered cone on an absolute scale, the incoherent background needs to be known. Since the cone of teflon cannot be resolved in the wide-angle setup, the teflon reference measurements can be considered to describe the incoherent background of the  $\text{TiO}_2$  samples. In doing so however, one neglects the different albedo of teflon with respect to the sample. The proper background for the sample,  $\alpha_{\text{inc,samp}}$  is therefore given by that of the reference,  $\alpha_{\text{inc,ref}}$  multiplied by the ratio of the albedos of sample and reference,  $A_{\text{samp}}/A_{\text{ref}}$ .

For an estimation of the albedos to a level of better than one percent, one needs to take into account losses at the sample/reference boundaries, as well as losses due to absorption. Up to now these losses have not been fully taken into account in the evaluation of the backscattering cones [18, 19].

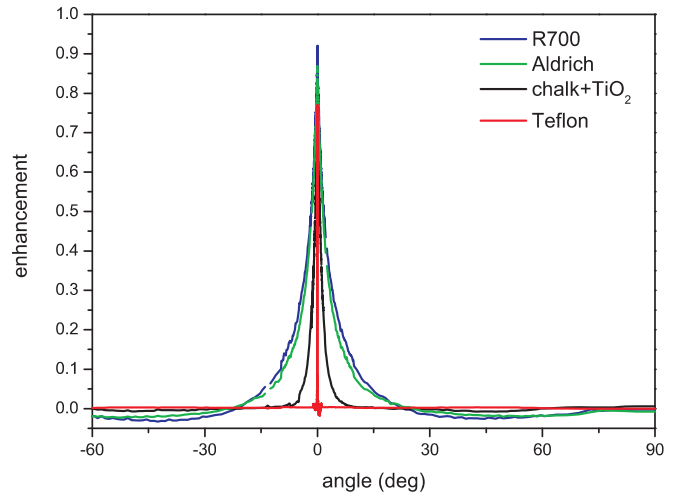


FIG. 2: Measurements of backscattering cones for different samples. As the cone width increases, more energy needs to be compensated. Thus the most turbid samples (R700 and Aldrich) lead to a noticeable energy cutback at angles around  $45^\circ$ . The amplitude of this cutback is reduced with decreasing turbidity, but stays positioned around  $45^\circ$ . This indicates that the cutback is due to effects occurring at a fixed length scale close to  $\lambda$ .

The loss due to leakage is estimated by comparing the diffuse energy in an infinite half-space at a certain time with the amount of energy that is left in a volume-cutout of the infinite half-space corresponding to the size of the reference [11]. This will neglect edge effects, but since we are only dealing with the very tails of the diffusive cloud, this will be accurate to the desired level. For this estimate, the diffusion coefficient of the sample/reference needs to be known. The loss factor for absorption can be calculated from the integral over the path length distribution  $P(D, \tau, t)$ , where  $D$  is the diffusion coefficient and  $\tau$  is the absorption time.

Both quantities needed to calculate the albedo,  $D$  and  $\tau$  can be determined with a time resolved transmission experiment [14, 20], see the inset of Fig. 1. Such a time of flight experiment directly gives the path length distribution inside the sample, which is a function only of  $D$  and  $\tau$ . In our experiment, the same dye laser is used in the backscattering experiments, thus making a possible wavelength dependence of  $D$  and  $\tau$  irrelevant. We thus calculate the ratio of the albedos using the absorption length  $L_a = \sqrt{D\tau}$  with respect to the reference and hence the absolute level of the incoherent background for all samples. Subtracting this background then directly gives a proper measure of the backscatter enhancement.

To represent cones with a wide variety of cone widths, we have used samples of ground  $\text{TiO}_2$  particles in its rutile structure with different particle diameters (R700: 245 nm and Aldrich: 540 nm), a mixture of  $\text{TiO}_2$  (R700) and ground chalk in a weight ratio of one to five, as well as solid teflon. The  $\text{TiO}_2$  particles are commercially avail-

able as pigment for white paint [14].

As can be seen in Figs. 1 and 2, a cutback of the backscattered energy is indeed observed when taking into account the different loss factors of reference and sample. This is most significant for samples with very wide cones like R700 and Aldrich with FWHM  $\approx 3.8^\circ$  and  $3.4^\circ$  respectively, where the enhancement is noticeably below zero for a range of  $50^\circ$  on both sides of the cone, as shown in Fig. 2. The  $\text{TiO}_2$ -chalk-mixture with FWHM  $\approx 1.5^\circ$  still shows a slight lowering of the enhancement, while the enhancement for teflon with FWHM  $\approx 0.013^\circ$  is essentially zero away from the cone. Note that unlike the coherent backscattering peak, the energy cutback is not characterized by a specific angle but it is rather spread out over the whole angular range. Furthermore, these energy cutbacks do compensate the energy enhancements of the cones, as the integral of the enhancement  $\alpha(\theta)$  over the backscattering half-space  $I = \int \alpha(\theta) \sin \theta d\theta$  is zero for all investigated samples within the margins of error. This shows that a determination of the absolute intensity scale is crucial for the correct observation of the backscattering cone. For such a determination, the different loss factors of reference and sample had to be accounted for.

Theoretically, the coherent backscattering cone has been described in great detail [17]. In the geometry of a semi-infinite medium of section  $S$  (see Fig. 3a), this description makes use of the following well-known expression for the coherent albedo  $\alpha_c^A$ ,

$$\alpha_c^A = \frac{c}{4\pi S l^{*2}} \int d\mathbf{r}_1 d\mathbf{r}_2 H^A(\mathbf{r}_1, \mathbf{r}_2) P(\mathbf{r}_1, \mathbf{r}_2) \quad (1)$$

where  $H^A(\mathbf{r}_1, \mathbf{r}_2) = e^{-\frac{\mu+1}{\mu} \frac{z_1+z_2}{2l^*}} e^{i(\mathbf{k}+\mathbf{k}') \cdot (\mathbf{r}_1-\mathbf{r}_2)}$  for an incident plane wave normal to the interface.  $P(\mathbf{r}_1, \mathbf{r}_2)$  is the probability of having a multiple scattering path starting at  $\mathbf{r}_1$  and ending at  $\mathbf{r}_2$ . The first factor in  $H^A$  describes the attenuation of an incident plane wave over a distance of the order of the elastic mean free path  $l^*$ . The second factor in  $H^A$  accounts for interference and leads to the enhancement with an angular width of order  $1/kl^*$ .

The interference term  $H^A$  is the product of four amplitudes describing the two incoming and the two outgoing plane waves. It is known as a quantum crossing and it is at the origin of coherent effects in quantum mesoscopic physics such as weak localization, universal conductance fluctuations and eventually it leads to the localization transition. Energy (or number of particles) conservation imposes constraints on the quantum crossings. It is well-known [16] that in order to fulfill this constraint, two other contributions  $H^{B,C}(\mathbf{r}_1, \mathbf{r}_2)$  must be added to  $H^A$ , which mix the in- and outgoing wave vectors. Energy conservation thus imposes that  $\int d\mathbf{R} (H^A + H^B + H^C) = 0$ , where  $\mathbf{R} = \mathbf{r}_1 - \mathbf{r}_2$ .

A complete description of coherent backscattering must therefore include these additional contributions  $H^B$  and  $H^C$ , which are equal. The physical basis of these contributions lies in a coupling of the light fields at the

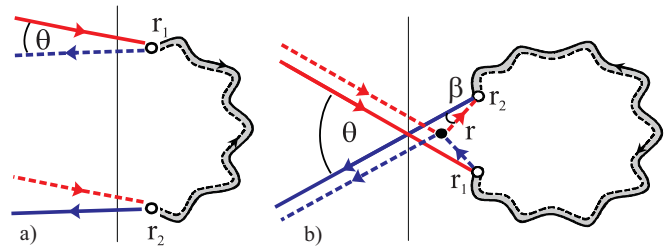


FIG. 3: Wave configurations of the contributions  $H^A$  and  $H^{B,C}$  to coherent backscattering.  $H^A$  (a) describes interference between time reversed amplitudes (full and dashed lines) and gives the classical cone shape [2]. When  $\mathbf{r}_1$  and  $\mathbf{r}_2$  are within a transverse distance of  $\lambda$ , the time-reversed loops have to be considered as closed and the amplitudes are becoming coupled. This is described by  $H^{B,C}$  (b), as an interference effect between the incident plane wave and the attenuated spherical wave traveling between the points  $\mathbf{r}_{1,2}$  and a newly introduced scatterer  $\mathbf{r}$  at an angle  $\beta$  (see text).

first and the last scatterer ( $\mathbf{r}_1$  and  $\mathbf{r}_2$ ), when they are within a volume of order  $\lambda^2 l^*$ . This coupling originates in an interference of the incoming plane wave with the multiply scattered spherical wave and is described by introducing an additional scattering event located in  $\mathbf{r}$  (see Fig.3b). This is reflected by the short range behavior of  $H^B(\mathbf{r}_1, \mathbf{r}_2)$  and the additional contribution results from almost closed diffusive trajectories. Consequently, this interference is not restricted to small angles  $\theta$  as is the case for  $\alpha_c^A$ . For the case of an incident wave normal to the interface, the contribution  $\alpha_c^B$  can be written as:

$$\alpha_c^B \simeq \frac{c}{S l^{*3}} \int d\mathbf{r} P(\mathbf{r}, \mathbf{r}) e^{-\frac{\mu+1}{\mu} \frac{z}{l^*}} h^2, \quad (2)$$

where

$$h \simeq - \int d\mathbf{r}' e^{i\mathbf{k}' \cdot \mathbf{r}'} \frac{e^{i\mathbf{k} \cdot \mathbf{r}'}}{4\pi r'} e^{-r'/2l^*} \simeq \frac{il^*}{2k} \quad (3)$$

is calculated to leading order in  $(kl^*)^{-1}$ . It is interesting to note the similarity between  $h$  and the shadow term which occurs in the optical theorem and ensures flux conservation for single elastic scattering. Here, the shadow terms  $h$  describe the interference between the incident and the multiply scattered waves. The integral in (2) can be solved approximately to give a correction  $\alpha_c^{B+C} \simeq -1.15(kl^*)^{-2} \mu/(\mu+1)$ . Thus the correction is of order  $-(kl^*)^{-2}$ . Noting that the angular integral of  $\alpha_c^A \simeq (kl^*)^{-2}$ , we indeed retrieve the energy conservation condition of quantum crossing, namely that the integral over  $\alpha_c^{A+B+C}$  is zero, as it should be.

The expression for  $\alpha_c^{B+C}$  shows that the interference effect in (2) is twofold. First,  $h$  is purely imaginary so that  $h^2$  is negative resulting in a depletion of the coherent albedo proportional to  $(kl^*)^{-2}$ . Secondly, this interference term does not contribute at a specific angular value but it is rather spread out over the whole angular range.

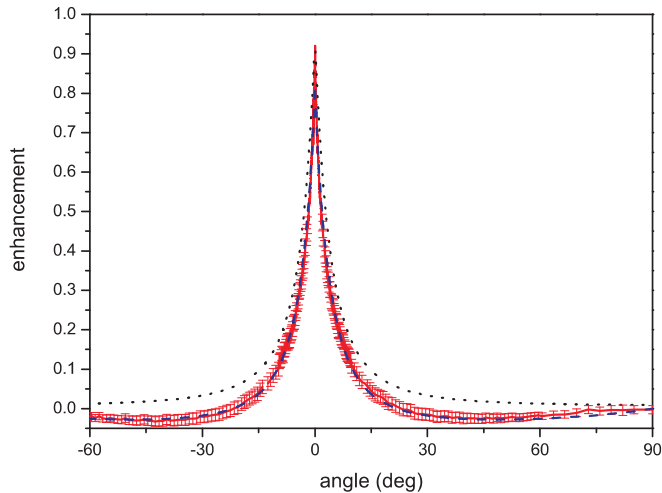


FIG. 4: Comparison of the backscattering cone of R700 with corrected and uncorrected enhancement. The agreement between the measured data and the fit of the corrected enhancement  $\alpha_c^{A+B+C}$  (dashed) is perfect within the errors. The uncorrected enhancement  $\alpha_c^A$  (dotted) calculated with the value of  $kl^*$  obtained by the fit of the data with  $\alpha_c^{A+B+C}$  describes the cone itself quite well, but shows significant deviations in the area of the energy cutback.

A fit of the total coherent albedo  $\alpha_c^{A+B+C}$  to our data is shown in Fig. 4 by the dashed line. The dotted line shows only  $\alpha_c^A$ , where the same value of  $kl^*$  has been used as in  $\alpha_c^{A+B+C}$ . Comparing this description with the uncorrected data in Fig. 1 shows that the  $kl^*$  values determined with those data are close to their real values.

In order to properly determine the turbidity of the sample, the value of  $kl^*$  obtained from (1) still has to be corrected for internal reflections [21], which lead to a broader distribution of light paths, and thus to a narrower cone. Furthermore, the ratio between the transport and elastic mean free paths will influence the pre-factor in the correction but is assumed to be close to unity.

In conclusion, we have shown experimentally that coherent backscattering does fulfill conservation of energy. To this purpose, the losses of the reference sample had to be quantified via a time of flight measurement to ensure an absolute energy calibration of the setup. If the loss of the reference differs significantly from the loss of the sample, this leads to different positions of the incoherent background in spite of equal incident laser energies.

Furthermore, we have provided a complete theoretical description of coherent backscattering based on the calculation of the three terms  $H^{A,B,C}$  that contribute to the Hikami box or quantum crossing.  $H^A$  describes the steep angular variation around backscattering and  $H^{B,C}$  take into account crossed diagrams dressed by a scattering impurity. Such an impurity provides an additional inter-

ference between incoming and multiply scattered waves at short distances. Since the cone is basically the Fourier transform of this intensity this leads to a broadly distributed energy cutback [10]. This improved description of the cone-shape for extremely turbid samples also allows a reliable determination of  $kl^*$  in such samples. A comparison of these result with those obtained previously on the same samples show however that the values of  $kl^*$  thus determined change only very little. This implies that the systematic dependence of deviations from classical diffusion is indeed as it was previously determined [13].

This work was supported by the Deutsche Forschungsgemeinschaft, the International Research and Training Group "Soft Condensed Matter of Model Systems", the Center for Applied Photonics (CAP) at the University of Konstanz, the Israel Academy of Sciences and by the Fund for Promotion of Research at the Technion. Furthermore, we would like to thank Aldrich and DuPont chemicals for providing samples used in this study. We also appreciate very much Peter Gross' help in building the backscattering cone setup.

- 
- [1] E. Fermi, Z. Phys. **88**, 161 (1934).
  - [2] E. Akkermans, P.E. Wolf, and R. Maynard, Phys. Rev. Lett. **56**, 1471 (1986).
  - [3] M. Kaveh *et al.*, Phys. Rev. Lett. **57**, 2049 (1986).
  - [4] M.P. van Albada, and A. Lagendijk, Phys. Rev. Lett. **55**, 2692 (1985); P.E. Wolf, and G. Maret, *ibid* **55**, 2696 (1985).
  - [5] B.W. Hapke, R.M. Nelson and W.D. Smythe, Science **260**, 509 (1993).
  - [6] E. Larose *et al.*, Phys. Rev. Lett. **93**, 048501 (2004).
  - [7] G. Bayer and T. Niederdränk, Phys. Rev. Lett. **70**, 3884 (1993).
  - [8] R. Dalichaouch *et al.*, Nature (London) **354**, 53 (1991).
  - [9] Y. Kuga and A. Ishimaru, J. Opt. Soc. Am. A, **1**, 831 (1984).
  - [10] E. Akkermans *et al.*, J. de Physique (France), **49**, 77 (1988).
  - [11] M.B. van der Mark *et al.*, Phys. Rev. B **37**, 3575 (1988).
  - [12] P.W. Anderson, Phys. Rev **109**, 1492 (1958).
  - [13] C.M. Aegerter *et al.*, Europhys. Lett. **75**, 562 (2006).
  - [14] M. Störzer *et al.*, Phys. Rev. Lett. **96**, 063904 (2006).
  - [15] M. Born and E. Wolf, *Principles of Optics*, Oxford University Press (1980).
  - [16] S. Hikami, Phys. Rev. B **24**, 2671 (1981).
  - [17] E. Akkermans and G. Montambaux, *Mesoscopic Physics of electrons and photons*, Cambridge University Press, (2007).
  - [18] P. Gross *et al.*, Rev. Sci. Instr. **78**, 033105 (2007).
  - [19] D.S. Wiersma, M.P. van Albada, and A. Lagendijk, Rev. Sci. Instr. **66**, 5473 (1995).
  - [20] G.H. Watson *et al.*, Phys. Rev. Lett. **58**, 945 (1987).
  - [21] J.X. Zhu *et al.*, Phys. Rev. A **44**, 3948 (1991).